Incorporating the gas flow in a numerical model of rf discharges in methane

A. Okhrimovskyy, A. Bogaerts,[a] and R. Gijbels
Department of Chemistry, University of Antwerp, Universiteitsplein 1, B-2610, Wilrijk, Belgium

(Received 12 January 2004; accepted 17 June 2004)

A two-dimensional modified fluid model for a capacitively coupled rf discharge in methane, used for the deposition of diamond-like carbon layers, is presented. The gas velocity calculated with a computational fluid dynamics code is used as an input for the modified fluid model. Convection is taken into account as an additional transport mechanism as well as diffusion and migration. The calculations show that the gas flow results in a shift of the maximum of the densities of the plasma species toward the grounded electrode. It is shown that this shift has a large effect on the fluxes of the ions and radicals toward the substrate where the deposition occurs. As a result, the deposition rate will increase if the gas velocity has a component directed to the surface and it will decrease in the opposite case. However, the uniformity of the layer can become worse when the convection velocity is too high for the reactor geometry studied here. © *2004 American Institute of Physics*. [DOI: 10.1063/1.1782951]

I. INTRODUCTION

The deposition of amorphous diamond-like carbon (DLC) layers has been increasingly used in recent years. The DLC thin films have important industrial applications because they are materials with unique properties such as extreme hardness, optical transparency, chemical inertness, high electrical resistivity, and thermal conductivity.[1] An effective way of fabricating the DLC is to utilize plasma-enhanced chemical-vapor deposition (PECVD) technology. In a plasma, different radicals that are essential for the deposition can be easily created. Microwave, pulsed, inductively coupled, or capacitively coupled rf discharges are used as plasma sources to assist the coating process.[2,3]

The deposition rate and the uniformity of the DLC layers are two important parameters for industrial applications of the PECVD method. They directly depend on the operating conditions of the process. The most significant input variables are the gas temperature and flow rate, pressure, and power applied to the discharge. The numerical modeling of the plasma is broadly used for finding optimal operating conditions and predicting the properties of the deposited films.

A number of numerical models of the gas discharge in methane were recently developed. Among them are the fluid models[4–8] and the particle-in-cell/Monte Carlo model.[9,10] The main difference in the fluid models is in the way of treating the electron kinetics. Some of them[4,5] use constant electron reaction rate coefficients; others calculate these coefficients on the basis of the Maxwellian[6] or the Druveysteyn[7,8] electron energy distribution functions (EEDF). A more accurate approach of calculating the electron reaction rates, based on the solution of Boltzmann's equation for the local value of the reduced electric field, was used in the past in the modeling of the radio-frequency discharge in silane-hydrogen[11] and methane-hydrogen[12,13] mixtures. The nonlocal effects were taken into account by the solution of a balance equation for the electron energy.

A one-dimensional and a two-dimensional comprehensive numerical model for a capacitively coupled rf discharge in methane for a PECVD reactor was developed in our group in recent years.[12,13] In this model, the neutral gas was assumed to be thermal and uniformly distributed throughout the reactor volume. The transport of charged plasma species was determined by diffusion and migration in the electric field, whereas the transport of the neutral species was only governed by diffusion. However, the gas flow is technologically an important part of the deposition process in industrial applications. Therefore, the gas flow needs to be incorporated in the plasma models to obtain reliable results.

Different methods are now being used for taking convection into account in gas discharge models. The program PLASIMO,[14] which was developed at the Eindhoven University of Technology can give a solution for the convection problem in the modeling of a gas discharge, but it is strongly limited in geometry (only tube or sphere-type geometry is applicable). The convection transport mechanism was also taken into account in inductively coupled plasma (ICP) models in chlorine.[15] In this work, a simplified model was used to investigate the effect of gas flow on the discharge. This model considers a plasma with only four species. The Maxwellian EEDF was taken as an approximation. The gas flow was included in the mass balance equation as a relaxation term with a gas residence time. This approach cannot show in detail the local effects of the gas flow on the plasma characteristics, which can be important for the question of the uniformity of the deposited layers. The models for ICP discharges in nitrogen with convection included were described in Refs. 16 and 17. The authors of Refs. 16 and 17 take into account four and five species in their model, respectively. The gas flow was included in the flux equation, but still the Maxwellian EEDF was used in both models to calculate reaction rates and transport coefficients.

[a]Electronic mail: Annemie.Bogaerts@ua.ac.be

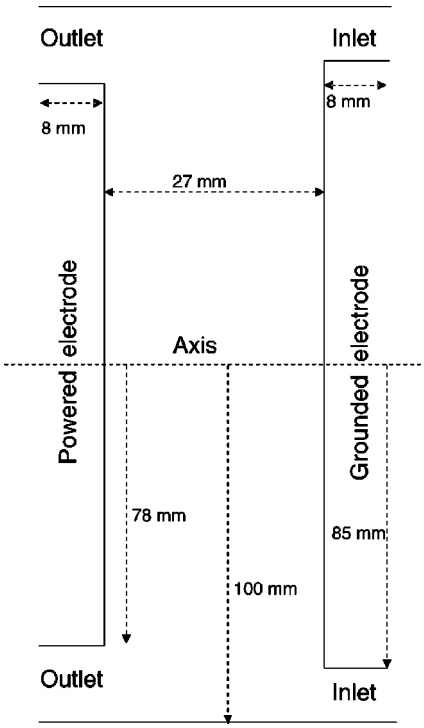

FIG. 1. Schematic picture of the reactor geometry.

A model for a dc discharge in argon with convection taken into account for a Grimm-type glow discharge ion source was developed in our group.[18] The main goal of the present work is to integrate the convection transport mechanism in the modeling procedure of a capacitively coupled rf discharge in methane for a real geometry of a PECVD reactor, based on the approach proposed before.[18] The present model is not restricted to a limited number of species taken into account and the EEDF can be non-Maxwellian. The effect of the gas flow on the discharge properties, and as a result on the deposition rate and the uniformity of the DLC layers, will be discussed in this paper.

II. DESCRIPTION OF THE MODEL

As mentioned earlier, a two-dimensional model for a capacitively coupled rf discharge in methane was previously developed in our group. The described model was used to simulate the discharge in a PECVD reactor of H-type geometry.[13] This is a cylindrically symmetrical reactor with an interelectrode distance of 2.7 cm. The inlet region is on the side of the grounded electrode whereas the outlet is on the side of the rf powered (13.56 MHz) electrode. A schematic picture of the reactor geometry is given in Fig. 1.

In the methane plasma, different species are created due to chemical reactions. Twenty species are taken into account in the model, among them are electrons, ions, radicals, molecular, and atomic species. The full list is presented in Table I.

In the model, 27 electron-neutral, 7 ion-neutral, and 12 neutral-neutral reactions are taken into account[12]. The Boltzmann equation is solved in the two-term approximation for the electron energy distribution function. This solution is used to find the rate constants of the electron-neutral processes and the electron transport coefficients as a function of an average electron energy. A detailed description of this procedure can be found in Ref. 12. The reaction rates of ion-neutral and neutral-neutral processes are considered to be constant and are taken from the literature (see Ref. 12).

TABLE I. List of species taken into account in the model.

Molecules	Charged particles	Radicals	Atom
CH_4, C_2H_4	CH_4^+, $C_2H_4^+$, CH_3^+	CH, C_2H_5	H
H_2, C_2H_6	H_2^+, $C_2H_5^+$, CH_5^+	CH_2	
C_2H_2, C_3H_8	$C_2H_2^+$, H_3^+, e	CH_3	

For every species, the balance equations for their densities are solved

$$\frac{\partial n}{\partial t} + \mathrm{div}(J) = S, \tag{1}$$

where J and S represent the mass flux and the sum of the chemical reaction rates of creation and destruction of the species of a particular type. The rates for electron-neutral processes are calculated in the EEDF part of the model mentioned earlier. The fluxes J are calculated in a drift-diffusion approximation. It means that in the case without a gas flow, the expressions for the fluxes are calculated from the following equation:

$$J = -D\nabla n + \mu n E, \tag{2}$$

where D and μ are the diffusion coefficient and the mobility of the species in the background gas, respectively, and E is the electric field vector. The Poisson equation for the electric field E is solved together with the mass balance equation for the electrons. The transport coefficients for the electrons are calculated in the EEDF part of the model, as it was mentioned earlier. The mobility μ is equal to zero for neutral species, and it is positive for positive ions and negative for electrons and negative ions (if the latter are present in the model).

The previous expression for the flux in Eq. (2) is also valid in the case of a moving gas with a uniformly distributed gas velocity U_{conv} when the reference frame is moved together with the gas flow. From it, the average velocities of a certain species in this reference frame can be calculated

$$v_{\mathrm{mv}} = \frac{J}{n} = -D\frac{\nabla n}{n} + \mu E.$$

If we go back to the laboratory coordinate system, we will get the expression for the average velocity of the species as the sum of the convection velocity U_{conv} and the average velocity v_{mv} in the moving frame

$$v_{\mathrm{lab}} = v_{\mathrm{mv}} + U_{\mathrm{conv}}.$$

From the last formula, we can obtain the expression for the fluxes of the species in case of a nonzero gas flow. For this, the average velocity of species in the laboratory system should be multiplied by the density of the species

$$J = -D\nabla n + \mu n E + nU_{\text{conv}}. \quad (3)$$

The modified flux expression in Eq. (3) has to be substituted in the balance equation as shown in Eq. (1). In case the convection velocity is not uniformly distributed, the local values of this velocity can be taken as an approximation.

The distribution of the convection velocity, U_{conv}, is calculated for the *H*-type reactor with computational fluid dynamics (CFD) software. We use the commercial code FLUENT (version 6.1.18). For our calculations, we assumed a laminar gas flow; a two-dimensional axisymmetrical approximation is used to model the methane/hydrogen flow in the reactor with this software. The chemistry was not included in the FLUENT calculations. Our estimations showed that it is not playing an important role in the formation of the mass-averaged velocity profile in industrially interesting cases. The balance equations for mass, impulse, and energy were solved together by using an implicit scheme.[19]

For this particular geometry and for a range of different boundary conditions (such as inlet gas flow rate and pressure at the outlet, etc.), the spatial distribution of the neutral gas density and the components of the velocity vector were obtained. The fields of gas temperature and pressure were calculated as well. The distribution of the mass-averaged velocity of the gas flow is used as an input in the modified fluid part of the model.

In principle, it is necessary to make a coupling back from the plasma model to the fluid dynamics code. Then, consecutive iterations have to be made until the convergence of the models. In a rf plasma, the buffer gas is heated according to Joule's law. This heating can be used as a source term in the energy balance equation in the gas flow model. A rough estimate of its effect on the gas flow was made by introducing a uniformly distributed power source based on the discharge input power. This estimation shows that for the conditions of interest, the effect of the gas heating in the plasma is negligible. The profiles of gas pressure, temperature, and velocity are not disturbed. For this reason, a complete coupling was not necessary in this work.

The described approach of including the convection as a new transport mechanism in a plasma model was previously used in the modeling of a dc discharge in argon.[18] It should be noted that the flux equations for the neutral species do not contain the densities of the species (only their derivatives) if no convection is included. It means that the balance equations for this type of species change their appearance when we incorporate a convection. Hence, in the present model, we now use the exponential Sharfetter-Gummel scheme[20,21] for neutrals as well as for charged species. This approach reduces the numerical instability during the calculations.

III. RESULTS OF THE MODEL

A. CFD calculations

The simulations have been carried out for a reactor of *H*-type geometry. The rf power is set to 5 W. The gas temperature at the inlet, outlet, and the wall temperature was set to 400 K. The pressure at the outlet was set to 20 Pa. The gas velocity at the inlet was taken as equal to 100 m/s unless mentioned otherwise. For this reactor, at the pressure and temperature mentioned earlier, it corresponds to 168 scss or about 10 slm. This is a high flow rate but still industrially relevant. Indeed, such a high gas flow rate is used, for instance, for the deposition of carbon-based thin films[22] and for other applications of plasma-based surface treatment.[23] The two-dimensional profiles of the axial and radial components of the gas velocity vector distribution are calculated with the CFD program.

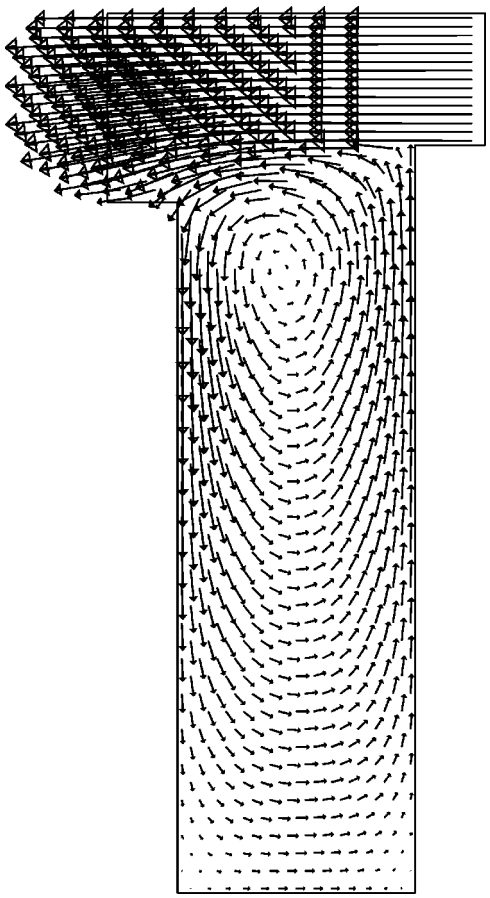

FIG. 2. Velocity vectors scaled by velocity magnitude. The maximum mass-averaged gas velocity is 102 m/s.

The axial velocity at this configuration is highest at the inlet-outlet regions. The value of it corresponds to the value of the velocity specified as a boundary condition of the inlet (i.e., 100 m/s) and it decreases by 15%–25% toward the outlet (i.e., to about 80 m/s). Inside the plasmas region, the axial velocity is much lower. It varies from −10 to +10 m/s, and it is equal to zero on the walls because of the boundary conditions.

The radial velocity is much lower over the reactor. It reaches maximum values of about 35–45 m/s near the edge of the powered and grounded electrodes and it is about zero in the middle of the plasma region. The value of radial velocity decreases away from the inlet-outlet regions toward the axis of the reactor, because of the symmetry boundary condition on the axis of the reactor.

The velocity vectors scaled by velocity magnitude are presented in Fig. 2. From this figure, one can see that for the *H*-type geometry the main part of the gas flow goes directly

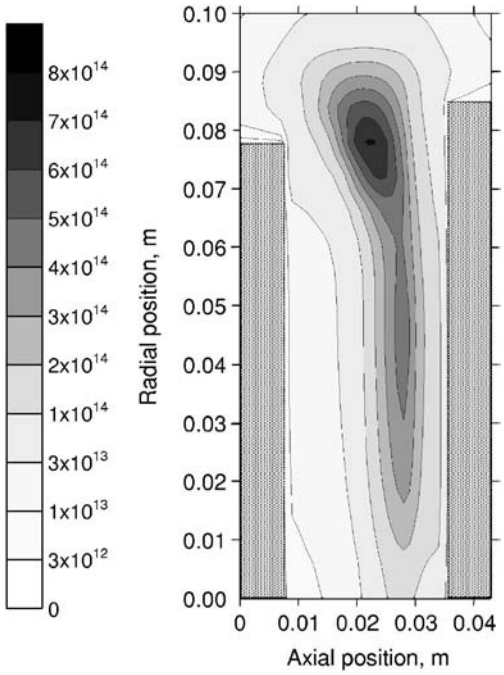

FIG. 3. Calculated time-averaged CH_5^+ two-dimensional density profile with convection included, m^{-3}.

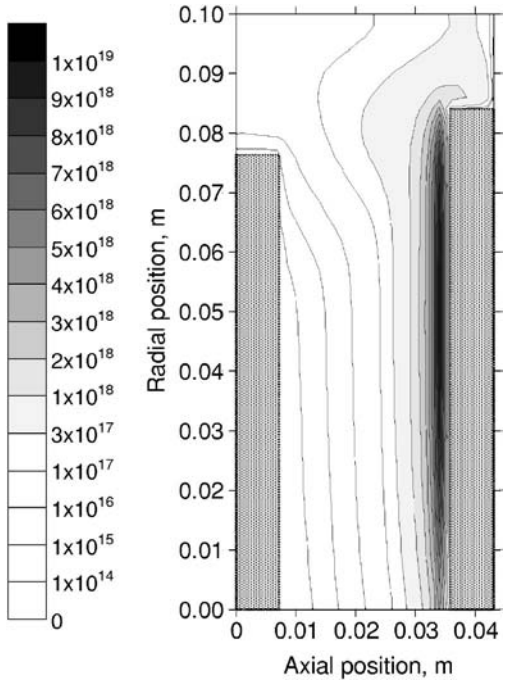

FIG. 4. Calculated time-averaged CH_3 two-dimensonal density profile with convection included, m^{-3}.

from the inlet to the outlet but some part of it penetrates into the plasma region and can influence the discharge characteristics. Note that in this geometry, the axial component of the velocity vector in the plasma region has the opposite direction from that in the inlet-outlet regions. As a result, the position of the maximum of the densities of the ions and radicals created in the plasma will be slightly shifted toward the grounded electrode.

At the condition under consideration, the variation of the gas temperature in the reactor does not exceed 0.5% and it corresponds to the specified inlet gas temperature and temperatures of the walls, which is equal to 400 K.

B. Plasma model calculations

As expected, the plasma model shows that the electric field near the electrodes is much higher than in the main part of the discharge. The corresponding values are about 100 kV/m in the sheaths and around 200 V/m in the bulk. At the pressure under consideration, the ion mobility is in the range of 1.5–3 m^2/Vs. From this, the ion-drift velocity can be estimated. For carbon-containing ions, we have about 300 m/s in the bulk. This is in the same order of magnitude as the applied gas velocity.

1. Density profiles of the species

The time averaged two-dimensional distributions of the densities of all species and the components of the electric field were calculated in the plasma model with convection included. The results of these calculations for the main ion species CH_5^+ are presented in Fig. 3. The density is highest near the side of the electrodes. The same result was observed before in a model without convection.[13] The peak value of the density is about 7.5×10^{14} m^{-3}. However, compared to the previous model, the distribution is shifted toward the grounded electrode. This happens because the gas flow moves the ions from halfway between the electrodes to the grounded electrode (see also Fig. 2). In the middle of the plasma region, the time-averaged density is about 5×10^{13} m^{-3}. Near the powered electrode the density is almost zero, near the grounded electrode it is about 1.5×10^{14} m^{-3}. The highest density gradients are also located near the grounded electrode. The densities of all other ions have the same behavior but with somewhat lower values.

The time-averaged density profile of the main radical CH_3 (Fig. 4) has the same behavior but the shift toward the grounded electrode is even more pronounced compared to the ionic profiles. Indeed, the ions are trapped by the electric field near the position of equilibrium and they can resist against the moving effect of the gas flow; whereas the neutral radicals are more influenced by the convection velocity. The maximum of the radical density (1.1×10^{19} m^{-3}) is obtained approximately in the same position in the radial direction as for the case where no convection was included[13] but, again, shifted toward the grounded electrode. It should be noted that analogous density profiles with lower values were obtained for the other radicals present in the model.

The shift effect of the particle density profile can be easily seen on the 1D plot of the density as a function of axial position. In Fig. 5, the calculated CH_5^+ ion-density profile at a distance of 6 cm from the reactor axis is presented as a function of axial position, for the cases when convection is included and not included. The ion density profiles for both cases look similar but they show a quantitative difference in the position and the value of the maximum. At this radial position, the density of CH_5^+ ions reaches its maximum when no convection is included. Adding a gas flow shifts this maximum in the direction of the grounded electrode. Be-

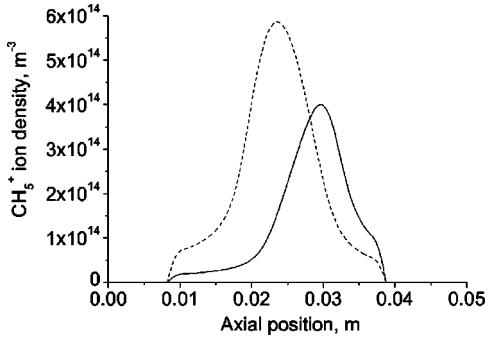

FIG. 5. Calculated time-averaged CH_5^+ ion density at a distance of 0.06 m from the axis, as a function of axial position with convection included (full curve) and not included (dashed curve).

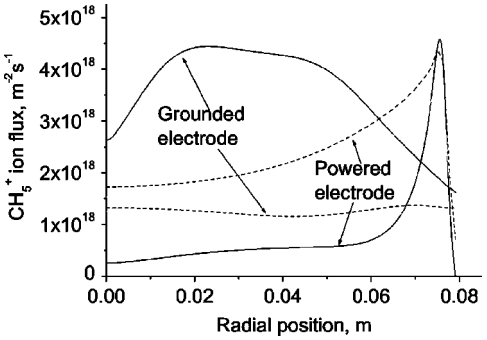

FIG. 7. Calculated time-averaged CH_5^+ ion flux toward grounded and powered electrodes as a function of radial position with convection included (full curve) and not included (dashed curve).

sides, at this radial position the gas flow also shifts the maximum of the density to the inlet-outlet areas. This is why the peak value is lower for the case when convection is included, compared to the case when it is not included. In Fig. 6, the axial cross section at the same radial position of the two-dimensional profile of the CH_3 radical density is presented for both cases (with convection included and not included). As it was mentioned before, the shift because of the gas flow is much more pronounced for radicals than for ions. Even more, the shape of the profiles is absolutely different. As a result of the gas flow, the radicals are compressed and their density profile has a sharp and high peak near the grounded electrode. Because the CH_3 radicals do not stick very well at the walls, they are not only shifted toward the grounded electrode but also blown out of the discharge area to the pumps and out of the reactor. This effect is easily seen by comparing the area under the curves in Fig. 6. It represents the overall numbers of CH_3 radicals in the discharge. For the case with convection included this area is much lower.

2. Ion fluxes and densities near the walls

For the purpose of deposition, the fluxes of carbon-based ions and radicals toward the depositing plates are much more important than their densities. The fluxes of all species to the powered and grounded electrodes were calculated in the plasma model with convection included. It is clear from Eq. (3) that convection cannot play a direct role for these fluxes, because the component of the convection velocity, perpendicular to the surface, is equal to zero according to the boundary condition (i.e., the gas cannot penetrate into the wall). To see the effect of the gas flow on the fluxes of the ions, we performed the calculations also with zero convection velocity, as it was made before in Ref. 13. The fluxes obtained in the calculations for both cases (with and without convection included) are presented in Fig. 7 for the main ion CH_5^+.

From this figure, one can see that at the earlier mentioned condition the gas flow plays an indirect role on the fluxes of ions. It is the result of the redistribution of their densities in the reactor. This effect can be seen in Fig. 8, which shows the radial dependence of the density of the CH_5^+ ions near powered and grounded electrodes. The redistributed density of the ions enters into the flux expression as a drift term in an explicit form. It means that this parameter can play a direct role for the fluxes of ions toward the wall. As shown in Figs. 3 and 5 the convection transport redistributes the ions in the reactor in such a way that their densities increase near the grounded electrode and this leads to increasing their fluxes toward this electrode. The fluxes to the powered electrode, on the other hand, are reduced due to the convection transport, for the same reason.

The ion flux profiles toward the grounded and powered electrodes for other ionic species, which can be involved in the deposition process, have the same behavior but with lower values.

3. Fluxes of neutral molecules and radicals near the walls

In the flux expression for the neutral molecules and radicals, we have only a diffusion term near the wall in the

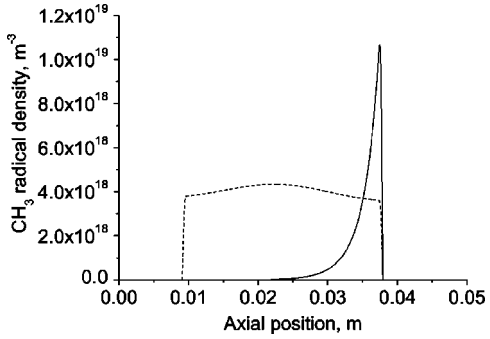

FIG. 6. Calculated time-averaged CH_3 radical density at a distance of 0.06 m from the axis, as a function of axial position with convection included (full curve) and not included (dashed curve).

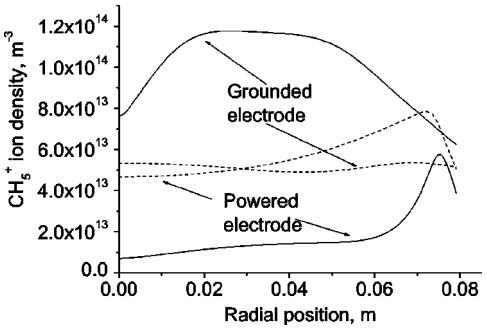

FIG. 8. Calculated time-averaged CH_5^+ ion density near grounded and powered electrodes as a function of radial position with convection included (full curve) and not included (dashed curve).

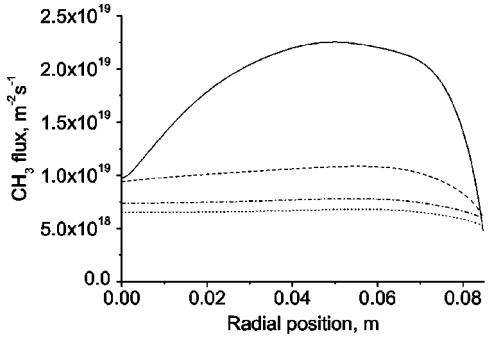

FIG. 9. Calculated CH_3 radical fluxes toward the grounded electrode as a function of radial position at different gas velocities U_{in} at the inlet: —100 m/s – – – 10 m/s, — · — 1 m/s, and …0 m/s.

direction perpendicular to the wall. It means that only gradients of the densities can affect the fluxes of the neutral radicals, which can be important for deposition.

To investigate the effect of the gas velocity at the inlet on the uniformity of the deposited layers, we compare the time-averaged fluxes of CH_3 radicals (i.e., the main radicals in the methane plasma) toward the grounded electrode calculated for the different gas velocities at the inlet. The result of this calculation is shown in Fig. 9. From this figure, one can see that with increasing the gas velocity at the inlet, the flux of this radical toward the grounded electrode increases. According to the flux equation, this increase can be only due to the indirect effect of the gas flow via the gradient of densities of these particles. With higher gas velocity at the inlet, the convection fluxes penetrate deeper into the reactor and cause a higher moving effect on the radicals by concentrating them near the grounded electrode. As a result, the gradient of the density of these particles at this position of the reactor also increases. The time-averaged flux of CH_3 radicals toward the powered electrode calculated at different gas velocities is presented in Fig. 10. The reduction of this flux with increasing gas velocity is even more pronounced than for the ionic flux. It happens because almost all radicals created near the powered electrode are shifted toward the grounded electrode. When the velocity at the inlet is equal to 100 m/s (not visible in Fig. 10) the calculated flux of CH_3 radicals becomes several orders of magnitude lower compared to the model without gas flow included.

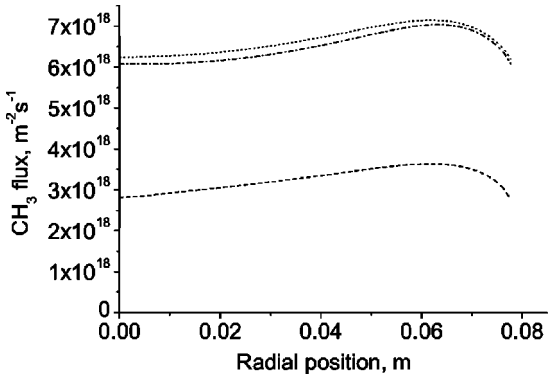

FIG. 10. Calculated CH_3 radical fluxes toward the powered electrode as a function of radial position at different gas velocities U_{in} at the inlet:-- -10 m/s —·—1 m/s, and …0 m/s.

The higher gradients lead to higher fluxes of the radicals toward the grounded electrode and hence a higher deposition rate of the layer. However, it can also be seen in Fig. 9 that the time-averaged flux of CH_3 particles towards the grounded electrode becomes less uniform near the axis of the reactor at high convection velocity. As a result, the uniformity of the deposited layers will be worse when the gas velocity at the inlet is too high. This happens because at higher convection velocities not only particles from the middle of the reactor are shifted toward the grounded electrode but in addition, the particles created near the axis are transported along the grounded electrode away from the axis toward the inlet (see Fig. 2).

IV. CONCLUSION

Based on the approach previously developed for dc discharges in Ar, the convection-transport mechanism of the plasma species was integrated into a model for capacitively coupled rf discharges in methane in a plasma enhanced CVD reactor of *H*-type geometry. Back coupling from the plasma model to the gas flow model was not necessary in this work, because the gas heating in the plasma is negligible for the conditions under consideration. The calculation shows that the gas flow has an important influence on the plasma characteristics in the case of a rf discharge. The density profiles and the fluxes to the walls of the carbon-containing ions and radicals, which play a role in deposition processes, are affected by convection. With increasing velocity at the inlet, the fluxes of these species toward the grounded electrode are increased. As a result, the deposition rate is also increased. However, the uniformity of the deposited layer can become worse when the convection velocity is too high. To improve the convection effect on the deposition rate, the geometry of the reactor should be changed in such a way that the convection can penetrate deeper into the reactor and the gas can shift the particles toward the wall, or the substrate, where they have to be deposited.

ACKNOWLEDGMENTS

A. Okhrimovskyy would like to acknowledge NATO for the financial support of this work. A. Bogaerts was supported by the Flemish Fund for Scientific Research (FWO-Flanders). This Research is also supported by NATO SfP project 974354. The authors thank W. Goedheer for many interesting discussions and D. Herrebout for supporting calculations for this work.

[1]J. Robertson, Adv. Phys. **35**, 317 (1986).
[2]E. Gogolides, D. Mary, A. Rhaballi, and G. Turban, Jpn. J. Appl. Phys., Part 1 **34**, 261 (1995).
[3]E. Dekempeneer, J. Smeets, J. Meneve, L. Eersels, and R. Jacobs, Thin Solid Films **241**, 269 (1994).
[4]N. Mutsukura, S. Inoue, and Y. Machi, J. Appl. Phys. **72**, 43 (1992).
[5]L. E. Kline, W. D. Partlow, and W. E. Bies, J. Appl. Phys. **65**, 70 (1988).
[6]A. Von Keudell and W. Möller, J. Appl. Phys. **75**, 7718 (1994).
[7]C. Cavalotti, M. Masi and S. Carrà, J. Electrochem. Soc. **145**, 4332 (1998).
[8]K. Bera, B. Farouk, and Y. H. Lee, J. Electrochem. Soc. **146**, 3264 (1998).
[9]K. Nagayama, B. Farouk, and Y. H. Lee, IEEE Trans. Plasma Sci. **26**, 125 (1998).
[10]V. Ivanov, O. Proshina, T. Rakhimova, A. Rakhimov, D. Herrebout, and

A. Bogaerts, J. Appl. Phys. **91**, 6296 (2002).
[11]G. J. Nienhuis, W. J. Goedheer, E. A. Hamers, W. G. Van Sark, and J. Bezemer, J. Appl. Phys. **82**, 2060 (1997).
[12]D. Herrebout, A. Bogaerts, M. Yan, R. Gijbels, W. Goedheer, and A. Vanhulsel, J. Appl. Phys. **90**, 570 (2001).
[13]D. Herrebout, A. Bogaerts, M. Yan, R. Gijbels, W. Goedheer, and A. Vanhulsel, J. Appl. Phys. **92**, 2290 (2002).
[14]G. Janssen, J. van Dijk, D. Benoy, M. Tas, K. Burm, W. J. Goedheer, J. van der Mullen, and D. C. Schram, Plasma Sources Sci. Technol. **8**, 1 (1999).
[15]D. P. Lymberopoulos, and D. J. Economou, IEEE Trans. Plasma Sci. **23**, 573 (1995).
[16]D. Bose, T. R. Govindan, and M. Meyyappan, J. Electrochem. Soc. **146**, 2705 (1999).
[17]Y. Tanaka and T. Sakuta, J. Phys. D **35**, 468 (2002).
[18]A. Bogaerts, A. Okhrimovskyy and R. Gijbels, J. Anal. At. Spectrom. **17**, 1076 (2002).
[19]Fluent 6.1 User guide (http://www.fluent.com).
[20]D. L. Sharfetter and H. K. Gummel, IEEE Trans. Electron Devices **16**, 64 (1976).
[21]J. P. Boeuf, Phys. Rev. A **36**, 2782 (1987).
[22]M. C.M. van de Sanden, M. F.A.M. van Hest, A. de Graaf, A. H.M. Smets, K. G.Y. Letourneur, M. G.H. Boogaarts, and D. C. Schram, Diamond Relat. Mater. **8**, 677 (1999).
[23]H. Barankova and L. Bardos, Science **174**, 63 (2003).